Bio-imaging with Functional Nano-objects

Noriaki Ohuchi*[1, 2)], Masaaki Kawai[1)], Yuu Sakurai[1)], Hideo Higuchi[3)], Yoshio Kobayashi[4)], Kohsuke Gonda[2)] and Motohiro Takeda[2)]

* Professor
1) Division of Surgical Oncology, Graduate School of Medicine
2) Division of Nano-Medical Science, Graduate School of Medicine
3) Department of Physics, Graduate School of Science, The University of Tokyo
4) Department of Biomolecular Functional Engineering, College of Engineering, Ibaraki University
E-mail: noriakio@mail.tains.tohoku.ac.jp

Abstract

Recent advances in engineering technologies of nano-materials are expected to be applied for medical field such as research on pharmacokinetics and novel therapeutic agents. A high- resolution *in vivo* 3D imaging method with very high-spatial accuracy was established, which enables visualization at the single molecular level. The movement of fluorescent nano-particles in a tumor interstitium and the membrane dynamics were measured in metastatic tumor cells using the *in vivo* imaging system. The therapeutic macromolecules such with sensing functions will be useful to increase therapeutic efficacy.

The dynamics of cell membranes based on their fluidity and morphology are crucial issues for cell motility during the invasion of cancer. A metastasis-activating factor in the cell membrane in stromal tissue of a living tumor in mice was labeled with antibody-conjugated quantum dots. The cells located away from vessels exhibited very slow diffusion velocity and no membrane protrusion was seen. In contrast, in the cells neighboring the vessels, the diffusion velocity was 10-300 times faster than that in cells far from the vessels. Moreover, the cells formed an invadopodia, a kind of pseudopodia, in the direction to the vessel. These results show that the cancer cells dramatically change their membrane fluidity during the metastatic process and form invadopodia to migrate directionally, suggesting potential targets for drugs to treat invasive tumors.

A novel contrast medium for X-rays and its distribution in the tumor was also examined. Nano-sized silica coated silver iodide beads exhibited contrast enhancement in the tumor for over one hour. Sentinel node navigation is an important clinical application for fluorescence nano-particles and silver iodide beads. The results in animal models demonstrate the potential of fluorescence and X-ray measurement as alternatives to existing tracers.

Future innovation in cancer imaging by nano-technology will provide extensive pharmaceutical and biological information, not only in clinical fields, but also in basic medical science.

1. Introduction

Highly engineered nano-materials are expected to be widely applied to medical diagnoses and treatments such as research on pharmacokinetics and novel therapeutic agents. Functional nano-particles include quantum dots (QDs), nano-micelle, nano-sized gold particles, silica coated silver iodide beads and oligo-dendrimers. They have unique properties and are potentially useful in medicine. On the other hand, the systemic distribution of the nano-materials is an important issue that should be determined for the establishment of safety.

Recent studies have proven the specific influence of particle size in malignancies because the tumor vessels have immature pores and increased permeability [1]. This phenomenon is called extended permeability and retention (EPR). So the size of nano-particles is an important parameter in the design anticancer drugs. The size of nano-particles is also important for sentinel node navigation surgery [2].

In cancer metastasis, cells first detach from the parent tumor, migrate and invade into surrounding connective tissue and blood vessels and then spread to other organs through the blood stream [3,4]. To move within tumor tissues, the cancer cells are thought to form the pseudopodia termed filopodia, lamellipodia and invadopodia, driven by actin polymerization, in the direction of cellular migration and invasion [5-9], thus indicating that the membrane dynamics play a fundamental role in cancer metastasis. To determine the membrane dynamics during metastasis, the understanding of *in vivo* membrane fluidity and morphology is very important. A trajectory analysis of membrane protein movement is one of best approaches to estimate membranous fluidity. The membrane protein randomly moves by passage between the compartments (40-700 nm) partitioned by actin filaments underneath the cell membrane (Fig. 1) [10-12]. The diameter of a filopodia is 100-200 nm [8]. Therefore, to intrinsically understand the membranous fluidity and morphology *in vivo*, imaging with at least several dozen nanometers-spatial resolution is essential.

Previous *in vivo* imaging using luciferase- or GFP-expressing cancer cells clarified the behavior of metastatic cancer cells in living mice [13-16]. However, since the spatial resolution in the imaging was at the micrometer-level, the details of the membrane dynamics in cancer cells *in vivo* are unknown. The bright and photostable QDs, fluorescence nanocrystals are useful for detecting the fluorescent signal with high-spatial resolution [17-19]. Previous studies succeeded in tracking anti-HER2 (human epidermal growth factor Receptor 2) monoclonal antibody-conjugated QDs *in vivo* [20].

This study was designed to clarify three applications of functional nano-particles. The first is to detect *in vivo* movement of nano-particles in the interstitium of a tumor, because the size may affect not only the accumulation of nano-particles but also the movement in the interstitium. The utility of functional nano-particles was established along with the development of novel optical measurement methods for both the nano-scale and macro-scale. The second goal was to develop a method to image tumor cell's membrane protein using antibody-conjugated QDs and visualize the details of membrane fluidity and morphology during metastasis with high-spatial resolution *in vivo*. The third application was to perform contrast enhancement of rat and tumor using a novel X-ray contrast media composed of silica coated silver iodide beads.

2. Materials and Methods

2.1. Nano-scale measurement of fluorescent nano-particles in the interstitium

2.1.1. Fluorescent nano-particles

'FluoSpheres®', which are polystyrene microspheres manufactured by Invitrogen, Molecular Probe (Oregon, USA) provided the particles 40 and 100 nm. The Quantum dot 705 ITK kit (Quantum Dot Corp., Hayward CA) was used for particles of 20 nm.

2.1.2. Cell culture and animal preparation

A human breast cancer cell line KPL-4 was kindly provided by Dr. J. Kurebayashi (Kawasaki Medical School, Kurashiki, Japan) [2]. KPL-4 cells were cultured in Dulbecco's modified Eagle's medium (DMEM) supplemented with 5% fetal bovine serum under 5% CO_2/air.

A suspension of KPL-4 (1.0 x 10^7 cells / 100 µl DMEM) cells was transplanted subcutaneously into the dorsal skin of female Balb/c nu/nu mice at 5 - 7 weeks of age (Charles River laboratories Japan, Yokohama, Japan). Several weeks after tumor inoculation, mice with a tumor volume of 100 - 200 mm^3 were used for the study. The mice were placed under anesthesia by ketamine and xylazine.

2.1.3. Measurement setup and detection of single particle movement

The optical system consisted of an epi-fluorescent microscope, Nipkow lens type confocal unit and an electron multiplier type CCD camera (Fig. 2). This system can capture images of single nano-particles at a rate of 33 ms/frame. The xy-position of the fluorescent spot was calculated by fitting to a 2D-Gaussian curve. A single fluorescent nano-particle could be identified by the fluorescence intensity. In addition, quantitative and qualitative information such as velocity, directionality and transport mode was obtained using the time-resolved trajectories of nano-particles.

The movement of nano-particles in the interstitium of the tumor was detected by the optical system after intravenous administration of fluorescent nano-particles.

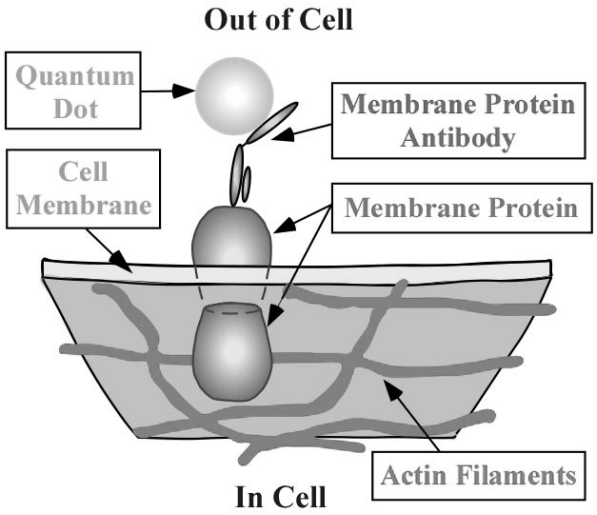

Fig. 1. A view showing a frame format of membrane protein labeled with its antibody-conjugated Quantum dot. The movement trajectory of membrane protein is known to be of temporally-confined diffusion type within domains partitioned by actin filaments underneath the cell membrane. The membrane protein randomly moves by hopping between the compartments. That indicates the diffusion velocity of membrane protein changes depending on the dynamics of actin filaments.

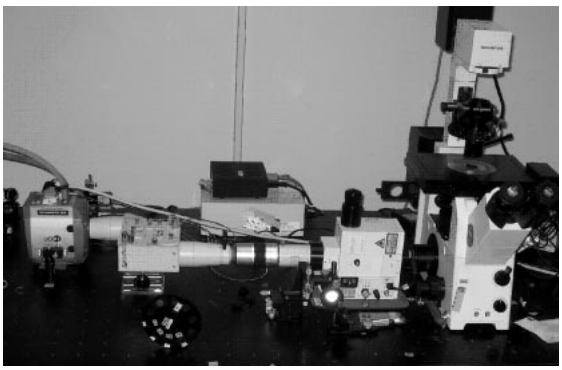

Fig. 2. The optical system with a confocal microscope and a hypersensitive CCD camera.

2.2. Imaging of cancer metastasis in living tumor

2.2.1. Membrane protein-antibody-conjugated QDs.

Membrane protein-antibody-conjugated QDs were prepared using a Qdot® 705 Antibody Conjugation Kit (Invitrogen) where the number indicates the emission wavelength.

2.2.2. Cell culture.

The metastatic human cancer cell line was cultured in DMEM (GIBCO) containing 10% FBS under 5% CO_2/air.

2.2.3. Optical system with a confocal microscope.

The optical system for observations of the fluorescence of QDs consisted primarily of an epi-fluorescent microscopy (IX-71, Olympus) with modifications, a Nipkow disk type confocal unit (CSU10, Yokogawa) and an electron multiplier type charge-coupled device camera (EM-CCD, Ixon DV887, Andor Technology; Fig. 1). The objective lens (X60, PlanApo, 1.40 NA, Olympus) was used for *in vivo* imaging. QDs were illuminated by a green laser (532 nm wavelength, CrystaLaser). The laser-excited fluorescence was filtered with a 685-725nm band-pass filter or >580nm long-pass filter. Images were taken at the rate of 5 frames per second. Moreover, in order to remove the oscillation of the heartbeat and respiration during the observation, a special stage was originally developed and attached to the above microscopy system.

Cancer cells (1 X 10^6) were suspended in 100µl L-15 (GIBCO) containing 10% FBS and transplanted subcutaneously into the dorsal skin of female SCID mice at 5-7 weeks of age (Charles River). Five to ten weeks after the transplantation, membrane protein-antibody-conjugated QDs were injected into tail vein of the mouse (Final concentration in blood is 5 nM). The mouse was placed under anesthesia with a mixture of ketamine and xylazine and the anesthetized condition was maintained within the course of the imaging session. Minimal surgery was performed to expose the living tumor by removing the skin, with as little damage to surrounding blood vessels as possible. The polyvinyl chloride plate (0.5 mm thickness) containing a small window (10 mm X 10 mm) was mounted on the exposed tumor and both were bonded by adhesive. The tumor-bearing mouse was fixed on a special stage, removing the oscillation, by fixation between the plate and stage and then observed. The position of the QDs on the tumor cell membrane was tracked using a previously described single molecule tracking method [19].

2.2.4. Mean square displacement analysis of QD movement.

To investigate the dynamic behavior of QDs, Mean Square Displacement (MSD) was calculated from x-y coordinates of individual tracking position data [20]. MSD values of individual tracking are defined by the following equation (Eq. (1)).

$$MSD(n\Delta t) = \frac{1}{N-n}\sum_{i=1}^{N-n}\left[(x_{i+n}-x_i)^2+(y_{i+n}-y_i)^2\right], \quad (1)$$

where x_i and y_i are positions on frame i, N is the total number of frames. Δt is the time between frames and distance between steps in time t and $n\Delta t$ is the time interval over which the MSD is calculated. Thus MSD is a function of time. To get the information for the diffusion coefficients and the velocities, MSD were fitted by the following equation (Eqs. (2) and (3)).

$$MSD(\Delta t) = 4D\Delta t + V^2(\Delta t)^2, \quad (2)$$

$$\lim_{t\to 0} MSD(\Delta t) = 4D\Delta t, \quad (3)$$

where D is diffusion coefficient and V is drift velocity.

When MSD was fitted versus time, the linear plot of MSD produced represents random Brownian movement. When the change in MSD was nonlinear with time, the movement is directed diffusion or confined diffusion. A decreasing slope indicates confined movement. On the other hand, directed diffusion produces an MSD plot with an increasing slope.

2.3. Contrast enhancement of a tumor by novel X–ray contrast media

2.3.1. Generation of silica coated silver iodide beads

The silica-coated silver iodide beads (AgI beads) of 40-80 nm were produced by the Stöber method. Potassium iodide and $AgClO_4$ was used for the formation of the silver-iodide core. Silica-coating of the fluorescent microspheres was carried out with ammonia-catalyzed reaction of tetraethylorthosilicate (TEOS) in ethanol–water solution. The ethanol solution of TEOS was added to aqueous PVP solution with stirring after addition of the suspension of the fluorescent microspheres. The hydrolysis of TEOS was initiated by addition of the aqueous ammonia solution to form a silica shell on the microspheres for 24 hr with stirring. Silica coated silver iodide nano-particles have a diameter of 40-80 nm [21].

2.3.2 Cell culture and animal treatments

A saline suspension of the silica-coated AgI beads was intravenously administered to rats with xenografts of human breast cancer (KPL-4). The CT images were sequentially acquired at 15, 30 and 60 min after intravenous administration.

These studies were carried out in accordance with the Institutional Animal Use and Care Regulations of Tohoku University, after receiving approval of the Committee on Animal Experiments.

3. Results

3.1. Nano-scale measurement of fluorescent nano-particles in tumors

The movement of single particles was observed in the perivascular, interstitial and intracellular regions of tumors. The particles could be successfully detected using the measurement system. The HER2 protein expressed in the cancer cells and its dynamics *in vivo* were visualized by QDs and fluorescence polystylene beads on a nano-scale. Fluorescent nano-particles of various sizes were also detected by the optical system. The perivascular region, interstitium and intercellular region in the interstitium of the tumor were investigated.

In the perivascular area, the 20 nm particles exhibited almost uni-directed movement by interstitial flow. In contrast, the 40 and 100 nm particles showed uni-directed movement with increased random diffusion.

In the tumor interstitial region, the movement of the 20 nm consisted of uni-directed movement and random diffusion. The 40 and 100 nm particles showed movement affected only by diffusion.

In the intercellular region, the 20 nm particle movement appeared to be highly restricted. The movement of the 40 and 100 nm particles appeared to represent only diffusion. That indicated Brownian motion.

3.2. Imaging of cancer cell dynamics in the living tumor

The goal was to understand the membrane dynamics during cancer metastasis. The phase contrast image and differential interference image could not be used *in vivo*. Therefore, the labeling of membrane protein with QDs was useful. To investigate whether this method allows visualization of the membrane microarchitecture in cells, the cultured cells were stained with membrane protein antibody-conjugated QDs. The fluorescent image of QDs showed spotty distribution in a single image with a 200 ms-exposure time. In the image, the outline of cell is not clear. However, since the membrane proteins move randomly on the cell membrane, the outline image of cell membrane could be obtained by making a superexposed image (200ms X 25 frames). When the fluorescent superexposed image and phase contrast image in the same cell were compared, the filopodia, a typical component of the cell microarchitecture, was observed in both images (Fig. 3), indicating this method is useful for visualization of membrane morphology *in vivo*.

Next, to image the membrane dynamics of metastatic cancer cells *in vivo*, a tumor-bearing mouse was prepared by transplantation of metastatic human breast cancer cells. Five to ten weeks later after transplantation, the membrane protein antibody-conjugated QDs was injected into tail vein of the mouse and then living tumor cells were observed following cancer metastasis: (1) in cells far from a blood vessel and (2) cells near a blood vessel.

(1) Cells far from vessels were visualized. In the cells, little active membrane dynamics was seen. The diffusion velocity of the membranous protein as typified by the white squares (Fig. 4) was 70 nm^2/s, which was 700-1500 times slower than that of the cells *in vitro* (data not shown). In Fig. 4, when a minimally-mobile particle was tracked, the standard deviation of the QDs-position was 17.2 nm for the X axis and 18.2 nm for the Y axis, indicating that this imaging method achieves < 18 nm-spatial resolution *in vivo*. In addition, in all of the *in vivo* imaging analyses, the most lateral QDs in the cell image superexposed over several seconds was defined as the QDs on the cancer cell membrane.

(2) Cells near a blood vessel were visualized. The cell formed an invadopodia, which plays a critical role in migration within the stromal connective tissue. The diffusion velocity of the membranous protein in the cells was 10-300 times faster than that of cells far from the vessels (Fig. 4). Moreover, in the cells near a vessel, the diffusion velocity on the invadopodia was 30 times faster than that on the other membranous regions in the same cell. These results suggest that, in the cells near vessel, faster diffusion velocity of membrane protein is involved in the invadopodial formation.

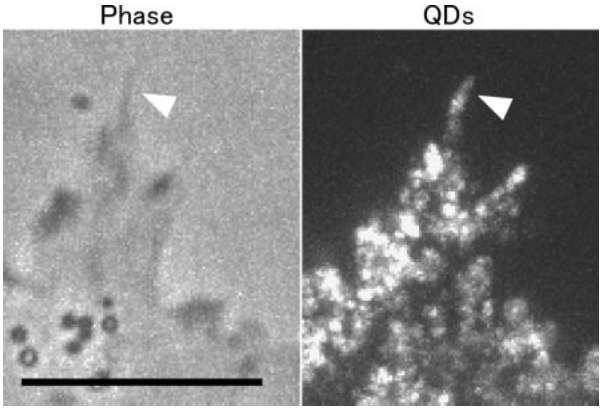

Fig. 3. Cultured cell labeled with membrane protein antibody-conjugated QDs. White arrow heads show a filopodia in a cell. Excitation was 532 nm. Emission was >580nm. Superexposured time was 5 s. Bar, 10nm.

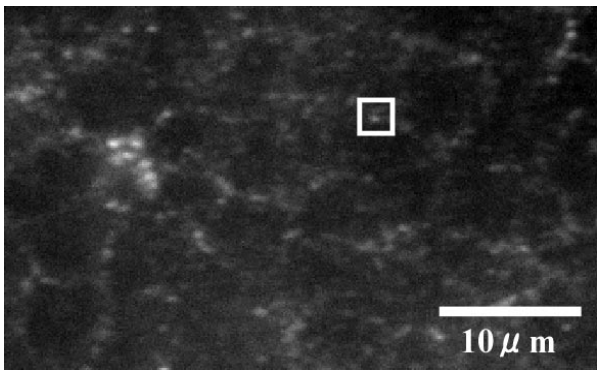

Fig. 4. Cells far from the blood vessels labeled with membrane protein antibody-conjugated QDs. A white square shows a representative image of QDs bound to membrane proteins on the edge of tumor cell. Excitation was 532 nm. Emission was >580nm. Exposure time, 0.2s.

3.3. Contrast enhancement of a tumor by novel X–ray contrast media

Enhancement of a tumor was visualized after administration of AgI beads. The Hounsfield number of the tumor gradually increased and achieved a maximum value in 60min and maintained contrast enhancement more than 24 hours.

4. Discussion

These studies captured the specific movement of nano-particles in various sizes in live mice after nano-particles had been injected into the tail vein of mice. In the former study, using anti-HER2 antibody-conjugated QDs, six stages of drug delivery are observed, 1) vessel circulation, 2) extravasation, 3) movement into the extracellular region, 4) binding to HER2 on the cell membrane, 5) movement from the cell membrane to the perinuclear region after endocytosis and 6) in the perinuclear region [20]. That study suggests that there are many stages to be considered for better drug delivery. The interstitium plays a very important role for drug delivery, because it is the scaffold of the tumor cells and the structure of the interstitium that defines the interface of tumor cells to drugs. The movement of the particles in each process was also found to be "stop-and-go", *i.e.*, sometimes the particles stay within a highly restricted area and then move suddenly after release. This indicates that the movement was promoted by a motive power and constrained by both the 3D-structure and protein-protein interactions. The motive power of the movement was produced by the diffusion force driven by thermal energy [2, 21, 22], interstitial lymph flow and active transport by motor proteins [23]. The cessation of movement is most likely induced by a structural barricade such as a matrix cage [2, 21, 22] and/or a specific interaction between proteins, *e.g.*, an antibody and HER2 [22], motor proteins and rail filaments such as actin filaments and microtubules [23]. That study strongly suggests that the size of drug carrier can be an important drug delivery modifier. If a carrier in size of 20 nm is used, it may reach cells soon and immediately diminish. Larger size can stay in the interstitium longer. Smaller particles can be used for drugs for treatment to allow drugs to access cancer cells. Larger particles can be used for the localization of a malignant lesion for surgical or radiological treatment.

There have been many different approaches to tumor-targeting "nanocarriers" including anti-cancer drugs, for passive targeting such as Myocet [23], Doxil [24] and for active targeting such as MCC-465 [25], anti-HER2 immuno-liposome [26]. The biological behavior of nano-carriers, including such crucial features as their transport in the blood circulation, interstitial behavior, cellular recognition, translocation into the cytoplasm and the final fate in the target cells, still remains poorly understood. These results suggest that the transport of nano-carriers can be quantitatively analyzed in the tumors of living animals by the present method.

The results of imaging of the cellular movement showed the cells far from vessels did not show active membrane dynamics. The reason for this might be that the amount of a membrane dynamics-activating stimulant, which is derived from blood component, is very low and of the region contains closely-attached cells and extracellular matrix that inhibit the membrane fluidity [27]. The cells near the vessel were attracted to vessel by the stimulant, formed a invadopodia in the direction of vessel. The concentration gradient of the stimulant through stromal extracellular matrix might induce formation of local invadopodia. Membrane fluidity on the invadopodia was 30 times faster than other membrane region. Since the diffusion velocity of membrane protein was controlled by compartmentalization by the actin filaments, the increased activity of actin dynamics in the invadopodia might decrease the compartmentalization and accelerate the diffusion velocity of the membrane protein.

The *in vivo* imaging in this study will allow researchers to achieve an intrinsic understanding of the membrane fluidity and morphology of metastatic cancer cells. These findings could be never presumed from only *in vitro* data. Therefore, this study opens new avenues for examination of biological phenomenon *in vivo*.

Silica coated silver iodide beads had contrast enhancement in a xenograft of breast cancer. In an earlier study, the slow increase in contrast enhancement of the liver and spleen was attributed to sedimentation of silica coated silver iodide beads in the capillary system. Enhancement of the tumor may therefore be attributed to EPR other than the sedimentation of silica coated silver iodide beads in the capillary system.

Conclusions

The fluorescent i*n vivo* imaging of nano-particles and antibody conjugated QDs was performed at a nano scale in mice. In addition, sentinel nodes were detected

by the silica coated fluorescent beads and contrast enhancement of the xeno-grafts of the tumor by silica coated silver iodide beads for X-CT in rats at a macro scale. Fluorescent single molecular measurement at the nano scale provides essential information for the development of drug delivery systems. In addition, CT images of tumor were acquired with novel contrast media with a unique advantage. Nano-materials for medicine would be a great aid to improve the made to order medicine by their highly sensitive and super selective property for diagnoses. Advanced sensing technologies such as single molecular imaging techniques are also required to make the best use of the functional nano-materials to achieve hyper sensitive and super selective imaging. These novel advanced nano-technologies may therefore revolutionize medicine in the near future.

Acknowledgements

The authors acknowledge the support of Tohoku University Global COE Program ‘‘Global Nano-Biomedical Engineering Education and Research Network Centre” and the Grant-in-aid for Research Project: Promotion of Advanced Medical Technology (H18-Nano-001) by Ministry of Health, Labour and Welfare.

References

[1] Dreher MR, Liu W, Michelich CR, et al. *J Natl Cancer I* **98**, 335-344, 2006.
[2] Kurebayashi J, Otsuki T, Tang CK, et al. *Br J Cancer* **79**, 707-717, 1999.
[3] Chambers AF, Groom AC, and MacDonald IC. *Nature Rev Cancer* **2,** 563-572, 2002.
[4] Schedin P. *Nature Rev Cancer* **6**, 281-291, 2006.
[5] Pollard TD and Borisy GG. *Cell* **112**, 453-465, 2003.
[6] Sahai E, Wyckoff J, Philippar U, Segall JE, Gertler F, and Condeelis J. *BMC Biotechnol* **5**, 14, 2005.
[7] Yamaguchi H, Lorenz M, Kempiak S, et al. *J Cell Biol* **168**, 441-452, 2005.
[8] Mattila PK and Lappalainen P. *Nature Rev Mol Cell Biol* **9**, 446-454, 2008.
[9] Sarmiento C, Wang W, and Dovas A. *J Cell Biol* **180**, 1245-1260, 2008.
[10]Sako Y and Kusumi A. *J Cell Biol* **125**, 1251-1264, 1994.
[11]Morone N, Fujiwara T, and Murase K. *J Cell Biol* **174**, 851-862, 2006.
[12]Andrews NL, Lidke KA, Pfeiffer JR, et al. *Nature Cell Biol*, 2008.
[13]Wang W, Wyckoff JB, Frohlich VC, et al. *Cancer Res* **62**, 6278-6288, 2002.
[14]Condeelis J and Segall JE. *Nature Rev Cancer* **3**, 921-930, 2003.
[15]Hoffman RM. *Nature Rev Cancer* **5**, 796-806, 2005.
[16]Jenkins DE, Hornig YS, Oei Y, et al. *Breast Cancer Res* **7**, R444-R454, 2005.
[17]Chan WC and Nie S. *Science* **281**, 2016-2018, 1998.
[18]Lidke DS, Nagy P, Heintzmann R, et al. *Nature Biotechnol* **22**, 198-203, 2004.
[19]Li-Shishido S, Watanabe TM, and Tada H. *Biochem Biophys Res Commun* **351**, 7-13, 2006.
[20]Tada H, Higuchi H, Wanatabe TM, and Ohuchi N. *Cancer Res* **67**, 1138-1144, 2007.
[21]Watanabe TM and Higuchi H. *Biophys J* **92**, 4109-4120, 2007.
[22]Kusumi A, Nakada C, Ritchie K, et al. *Annu Rev Biophys Biomol Struct* **34**, 351-378, 2005.
[23]Kross M, Niemann B, Massing U, et al. *Cancer Chemother Pharmacol* **54**, 514-524, 2004.
[24]O'Brien ME, Wigler N, Inbar M, et al. *Ann Oncol* **15**, 440-449, 2004.
[25]Hamaguchi T, Matsumura Y, Nakanishi Y, et al. *Cancer Sci* **95**, 608-613, 2004.
[26]Park JW, Kirpotin DB, Hong K, et al. *J Control Release* **74**, 95-113, 2001.
[27]Yamaguchi H, Wyckoff J, and Condeelis J. *Curr Opin Cell Biol* **17**, 559-564, 2005.